

1 **Robust Optimization for Stability of I-Walls and Levee System**
2 **Resting on Sandy Foundation**

3 **Nadarajah Ravichandran^a, Lei Wang^{b*}, and Parishad Rahbari^c**

4 ^aGlenn Department of Civil Engineering, Clemson University, Clemson, SC 29634, United States,
5 nravic@clemson.edu

6 ^bDepartment of Civil Engineering, University of the District of Columbia, Washington, DC 20008,
7 United States, lei.wang@udc.edu (*Corresponding author)

8 ^cGlenn Department of Civil Engineering, Clemson University, Clemson SC 29634, United States,
9 prahbar@g.clemson.edu

10 **ABSTRACT**

13 During Hurricane Katrina in 2005 and the events thereafter, failures of levees with I-walls
14 caused extensive flooding and damage. The geological background in the New Orleans area and
15 associated uncertainties contributed significantly to the failures. To increase the robustness of the
16 I-walls and levee system and reduce the associated risk of failure, the uncertainties of the system
17 must be incorporated into the design procedures, especially in a geological environment mainly
18 composed of sand deposits. This paper presents a robust optimization procedure to identify optimal
19 designs for the stability of an I-walls and levee system supported on sandy foundation soil in the
20 face of flood hazards. The uncertainties associated with the I-walls and levee system, including
21 the strength parameters of levee and foundation soils and the height of the floodwater behind the
22 I-walls, were considered in a systematic manner. The wall embedded depth, levee crown width,
23 and slope ratio of the levee in the landside were considered as the design parameters. For the robust
24 optimization, the construction cost of the I-walls and levee system and the standard deviation of
25 the failure probability were considered as the design objectives. Finally, the multi-objective
26 optimization resulted in a set of acceptable designs that were presented in a graphical form called
27 Pareto front, which is combined with the knee point concept to provide useful decision aids for
28 selecting the most preferred design that meets both the economics and performance requirements.

29 **Keywords:** Uncertainty; Levee; Stability; Robust Optimization; Finite Element Method

30

31 **1. INTRODUCTION**

32 Typically, levees with or without floodwalls are designed using deterministic methods
33 considering the site-specific geotechnical and extreme hydrological parameters. The conventional
34 approaches for designing such hurricane protection systems are typically based on the performance
35 of an individual component of the system, and the factor of safety is used to address the
36 uncertainties in such design approaches (Sills et al. 2008). Therefore, a more comprehensive
37 probability-based approach that integrates the individual components of the system is needed to
38 evaluate the impacts of the uncertainties on the system performance. In this study, a response-
39 surface-based probabilistic design approach was developed and implemented to systematically
40 account for the uncertainties and quantify the failure probability of the system and the associated
41 variations. The approach can explicitly incorporate the reliability, robustness, and cost-efficiency
42 of the design in the optimization process.

43 The sudden and uncontrolled failure of critical levee systems may result in severe flooding
44 which causes significant economic and human losses (Flor et al. 2010; Yang et al. 2011). The
45 failure of such systems usually occurs due to the exceedance of water elevation above the levee
46 crown and/or overestimation of the strengths of levee and foundation soils. However, increasing
47 the capacity of such flood protection systems and protecting the landside from the overflow of
48 water can be achieved through expanding the levee section or floodwall installation. Expanding
49 the levee section is not considered as a reasonable option where there is a limited right of way on
50 the landside or the existing foundation is not suitable for additional levee load. Fig. 1 shows the
51 levee section and the additional space needed to expand the levee section which may not be

52 available in many situations. In such situations, a floodwall is commonly used to increase the
53 capacity of the levee.

54 There are two types of floodwalls, as shown in Fig. 2: I-walls and T-walls. The I-walls are
55 I-shaped walls typically consisting of sheetpile walls driven into the levee and concrete caps fixed
56 to the top of the sheet piles above the levee crown. The T-walls are like gravity-cantilever retaining
57 walls that resist the flood load by cantilever action. Because of the complexity in the design and
58 construction of T-walls, I-walls are commonly used in practice.

59 Flooding caused by the failure of an I-walls and levee system protecting highly populated
60 and high-valued real estate areas can be significant. The flooding caused by the levee failures after
61 Hurricane Katrina resulted in billions of dollars in damage in New Orleans. Particularly, flooding
62 in some areas was caused by the failure of I-walls and levee systems supported by the sandy
63 foundation. It was also found that the geological history and depositional environment significantly
64 affected the mechanical and flow properties of the foundation soil beneath the I-walls and levee
65 system (Dunbar and Britsch 2008). Sills et al. (2008), Duncan et al. (2008), and the IPET
66 (Interagency Performance Evaluation Taskforce) team investigated the failure mechanisms of I-
67 walls and levee systems during Hurricane Katrina. They reported that the I-walls and levee system
68 of the South London Avenue failed largely due to the piping that occurred in the sandy foundation.
69 Centrifuge tests were conducted to evaluate the failure mechanism of the I-walls and levee system
70 (Sasanakul et al. 2008 and Ubilla et al. 2008), and it is found that the layout of the levee geometry,
71 the embedded depth of I-walls, and engineering characterization of soils contributed to the failure
72 of the levee. It was recommended to increase the embedded depth of the sheet pile to increase the
73 lateral support of the wall and decrease the flow of water through the sandy foundation.

74 In addition to the IPET, the ILIT (Independent Levee Investigation Team) also conducted
75 a comprehensive site investigation and computer analyses on two-dimensional levee sections from
76 several locations where I-walls and levee system failures were observed (Seed et al. 2008). The
77 teams (IPET and ILIT) developed simplified two-dimensional cross-sections of the I-walls and
78 levees found at the breach locations and analyzed them using the soil properties and storm-surge
79 data measured from the site. They used coupled geotechnical-hydrological finite element software
80 PLAXIS and limit equilibrium software. For the limit equilibrium analysis, IPET used SLIDE and
81 UTEXAS and ILIT used SLOPE/W. Although these studies provide recommendations based on
82 limited experimental and simplified numerical studies, a comprehensive study considering the
83 uncertainties associated with the properties of the system and loading in the design of I-walls and
84 levee systems is required. Also, the risk-based optimization studies conducted in the past only
85 considered the uncertainties associated with the flood load. Moreover, most of the past levee
86 design optimization procedures considered failures due to overtopping, and a few studies have
87 included the geotechnical failure of the levees (Tung and Mays 1981; Hui 2014).

88 A reliable and robust design approach must not only consider I-walls, levee, and foundation
89 as a single system but also consider the uncertainties associated with the system. Therefore, a
90 probabilistic design approach needs to be implemented to achieve the reliability and robustness of
91 the system. The reliability is ensured by evaluating the calculated failure probability to make sure
92 it is less than the acceptable failure probability. Also, the robustness of the system refers to the
93 reduction of design sensitivity to the effect of uncertainties in the system (Gong et al. 2014; Yu et
94 al. 2019; Tan et al. 2020). Furthermore, the cost is explicitly considered as one of the design
95 objectives to ensure the economics of the design. Generally, the cost is balanced with safety
96 requirements using the factor of safety for the stability of the system in conventional deterministic

97 design approaches while using the allowable failure probability in probabilistic design approaches.
98 This paper provides a robust design scheme to optimize the cost and robustness of the I-walls and
99 levee system, and the results of the robust design were compared with the non-robust design
100 results. Also, for demonstrating the effect of variation of water elevation behind the floodwall on
101 the I-walls and levee system design, several parametric studies were carried out considering the
102 safety and failure probability.

103 **2. DESIGN PROBLEM FOR STABILITY OF I-WALLS AND LEVEE SYSTEM**

104 **Defining the Problem and the Variables of the Study**

105 For demonstrating the proposed design approach, an I-walls and levee system with clayed
106 soils as levee materials and the sandy deposits as the underlying foundation was used in this study
107 (Fig. 3). The levee crown cover materials are lime-treated clayed soils with negligible erodibility.
108 The floodside slope materials are well-compacted clayed soils with high plasticity, which has very
109 low to negligible erodibility. The key factors affecting the system performance include both the
110 design parameters and uncertain variables. The design parameters considered in this study are the
111 embedded depth of I-walls (D), the levee crown width (X), and the slope ratio of the levee landside
112 (S). The wall height beyond the crown of the levee (H_{ex}) is 2 m and the slope ratio of the floodside
113 of the levee is 2H:1V. The uncertain parameters (also known as random variables) considered in
114 the I-walls and levee system, including floodwater elevation behind I-walls (wl), undrained
115 strength of the clayed levee soil (s_u), and angle of friction of the foundation soil (ϕ). Further details
116 of the ranges and statistical properties of the variables are discussed in the following sections.

117 **Design Parameters for Stability of the I-Walls and Levee System**

118 One of the critical parameters for the I-walls and levee system's design is the embedded

119 depth of the I-walls that has significant effects on the stability of slopes, control of seepage, and
120 cost of construction. In deterministic design, to ensure that adequate embedded with considering
121 the variations in soil properties, the minimum embedded depth (D) of the sheet pile wall shall be
122 the greatest of 2.5 times the exposed height of the I-walls (H_{ex}) and 3 m below the levee crown
123 (EC 1110-2-6066). The maximum value of H_{ex} is typically limited to 2 m for I-walls on levees or
124 in soft soils (EC 1110-2-6066). Thus, in this study H_{ex} was kept remained constant at 2 m, and the
125 lower and upper limits of D were assumed to be 2 m that is equal to H_{ex}) and 8 m, respectively
126 (Rahbari 2017).

127 The levee crown width (X) was considered as another design variable due to its effect on
128 slope stability. The lower and upper limits of X were assumed to be 3 m and 6 m, respectively. It
129 should be noted that the same elevation (horizontal crown) was assumed for the flood side and
130 landside of the levee crown in this study. The other design variable of the study is the landside
131 slope of the levee. For levees made of clay and riverine levees in which the wave action is
132 insignificant than the coastal levees, a steeper flood side can be used (EM-1110-2-1913).
133 Therefore, the slope ratio of the floodside was fixed at 2H:1V and slope ratio of the landside (S)
134 was varied between 2H:1V and 4H:1V. The design parameters of this study and their ranges are
135 tabulated in Table 1.

136 **Random Variables for Stability of the I-Walls and Levee System**

137 The uncertainties in I-walls and levee system design arise from both resistance to failure
138 and load. These include shear strength, deformation, and hydraulic parameters of the levee fill and
139 foundation soils and the floodwater elevation. Since the levee fill and foundation soils are different
140 in this study, the uncertainties associated with both soils must be considered. Among the many

141 parameters, the undrained strength (s_u) of the clayed levee material and the angle of friction of the
142 sandy foundation (ϕ) were considered as the soil-related uncertain parameters in this study. The
143 floodwater elevation (wl) above the levee crown was considered as the loading-related random
144 variable. The floodwater elevation varies between 0 and 2 m above the crown of the levee based
145 on the limiting value of H_{ex} of 2 m. The statistical values for uncertain variables are listed in Table
146 2. The standard deviation values reported in Table 2 are determined based on the three-sigma rule
147 and the range of the uncertain variables (Duncan 2000; Rahbari and Ravichandran 2018; Gao et
148 al. 2019).

149

150 **3. STABILITY ANALYSIS OF I-WALLS AND LEVEE SYSTEM**

151 **Stability Analysis Methods**

152 Several limit equilibrium-based (LE-based) methods are available in the literature for
153 evaluating the stability of an earth slope. These methods provide a factor of safety against failure
154 (Coduto 1999; Chen et al. 2019). Between the mass procedure and method of slices, the method
155 of slices is popular for computing the factor of safety of slopes with complex geometries and soil
156 conditions. Among the many methods that utilize the method of slices, the Spencer method is used
157 in this study.

158 Although the limit equilibrium-based methods provide a factor of safety against sliding
159 and it is easy to conduct simulations, they do not provide any information about the deformation
160 of the slope. Understanding the deformation behavior of levees, especially with floodwalls, is
161 important because it can lead to the failure of the floodwall and result in the complete failure of
162 the flood wall and levee system. In such situations, a finite element-based (FE-based) approach

163 can be utilized to gain further insights into the behavior of the levee-floodwall system. The finite
164 element-based method has become popular and widely for slope analysis that can provide realistic
165 results in terms of system deformation and slope failure mechanism (Liu et al. 2018; Gao et al.
166 2019). In other words, finite element-based analyses are useful when it is necessary to capture the
167 behavior of the soil and wall in a coupled manner with complex loading and geometric conditions.
168 In the finite element-based programs, the slope failure occurs naturally in the system where the
169 soil shear strength is unable to resist the shear stress (Griffiths and Lane 1999). One of the main
170 FE-based slope stability analysis methods is known as the strength reduction method, in which the
171 critical slip surface is sought based on shear strain increase due to the reduction in shear strength
172 of soil (Chen et al. 2014).

173 Therefore, to analyze the overall stability and performance of the I-walls and levee system
174 resting on the sandy foundation, both the FE-based program PLAXIS 2D and the LE-based
175 program SLIDE were used in this study. The comparison of results obtained from these programs
176 allows for evaluating the accuracy of the FS values, which can accordingly guarantee the accuracy
177 of the failure probability computations. Thus, selected designs of the I-walls and levee system were
178 chosen based on the feasible design domain and were simulated using the FE-based program
179 PLAXIS 2D and the LE-based program SLIDE. The overall stability using PLAXIS 2D is
180 computed through safety analysis in which the strength reduction method is applied for obtaining
181 FS following the consolidation and plastic analyses. On the other hand, Spencer's method can be
182 used for FS calculation in SLIDE (Rocscience 2016), which is a LE-based slope stability software
183 with built-in finite element groundwater seepage analysis.

184 **Stability Analyses Using LE and FE Procedures**

185 In this study, the overall stability of the levee-floodwall system resting on a sandy

186 foundation was evaluated using both the FE-based program PLAXIS 2D and the LE-based
 187 program SLIDE. For the LE-based analysis, Spencer's method implemented in SLIDE software
 188 was used. In the calculation, the soil mass above the slip surface is divided into a number of slices
 189 and both moment and force equilibrium of the sliding mass are satisfied in the analysis. A number
 190 of iterations are needed to locate the critical slip surface and ensure the complete equilibrium to
 191 obtain an accurate factor of safety. In SLIDE modeling, the stress-strain behavior of levee fill and
 192 the foundation soil was represented by Mohr-Coulomb material model, and the Infinite Strength
 193 material type was used for I-walls to treat the wall as a rigid component. For modeling steady-state
 194 seepage conditions, hydraulic boundary conditions were applied by setting the total heads at the
 195 flood side and landside of the levee system. The finite element seepage analysis for the steady-
 196 state condition is built into the SLIDE program. The simulation domain was spatially discretized
 197 into around 1000 elements using 6-node triangular elements. A sample SLIDE model of the levee-
 198 floodwall system is shown in Fig. 4.

199 For the stability evaluation using the finite element method implemented in PLAXIS 2D,
 200 the strength reduction method was adopted to assess the global FS (factor of safety) of the I-walls
 201 and levee system (Brinkgreve et al. 2015). In the strength reduction method, the shear strength
 202 parameters ($\tan \phi$ and c or s_u) of the soil are successively reduced until failure of the system occurs.
 203 The total multiplier $\sum Msf$ is used to define the value of the soil strength parameters at a given
 204 stage in the analysis:

$$205 \sum Msf = \frac{\tan \phi_{input}}{\tan \phi_{reduced}} = \frac{s_{u,input}}{s_{u,reduced}} \quad (1)$$

206 where the strength parameters with subscript *input* refer to the properties entered in the material
207 sets and those with subscript *reduced* refer to the *reduced* values used in the analysis. $\sum \text{Msf}$ is set
208 to 1 at the start of the calculation to set all material strengths to their input values. The value of
209 $\sum \text{Msf}$ at failure is considered as the FS of the system. Selecting a point in failure zone of the
210 system, the FS curve can be plotted and the global FS can be determined (Brinkgreve et al. 2015).

211 The soil behavior in the finite element model was modeled using Mohr-Coulomb models
212 and I-walls were modeled using linear elastic models (e.g., plate element for the sheet pile
213 component and soil polygon for the concrete cap). The soil-wall interaction is incorporated in the
214 modeling using interface elements. The concrete cap dimensions were obtained from the reports
215 on the levee I-walls of London Ave canal in New Orleans, as shown in Fig. 5, which was also
216 constructed on the sandy foundation (Burk & Associates, Inc. 1986). For the sheet pile wall
217 material, properties of PZ-27 sheet pile were used, and the plate parameters in PLAXIS 2D were
218 computed accordingly as listed in Table 3. Using Young's modulus (E) of steel, moment of inertia
219 (I) value and the cross-sectional area (A) of the section PZ-27, the equivalent thickness (d) of the
220 wall can be calculated to be implemented in PLAXIS 2D, considering h as the plate thickness and
221 b as the plate width (=1m). Moreover, finite element models consisting of very fine finite element
222 meshes with over thousands of triangle elements. A sample finite element model is shown in Fig.
223 6.

224 It should be noted that before performing the stability analysis using LE and FE procedures,
225 nine subset designs, as listed in Table 4 based on the range of parameters in the design domain,
226 were selected as design parameters. Regarding the simulation setups, the FS values of the I-walls
227 and levee system were obtained using both methods for variations of design variables (min., mean,
228 max.) and compared, as shown in Fig. 7. It can be observed that the two methods are in good

229 agreement with each other. However, the results of PLAXIS 2D were adopted in the optimization
230 approach of this study, as is discussed in the following sections.

231 **Evaluating the Effect of Uncertainties on Stability of the I-Walls and Levee System**

232 The effect of uncertainties (random variables) of the system (wl , ϕ and s_u) on the factor of
233 safety (FS) of the I-walls and levee system was investigated in this section. For subset designs in
234 Table 3, the variations of FS with a change in each random variable are displayed in Figs. 8-10.

235 It can be observed from these figures that the FS value is greater than the assumed
236 minimum FS of 1.5 in all selected design combinations. However, the worst design combinations
237 are not considered here for monitoring the effect of limiting values of each design variable
238 independent from the other two design parameters. Overall, Figs. 8-10 show that I-walls and levee
239 systems were more stable with greater depth of wall embedded, wider crown levee, and milder
240 landside levee slope. Fig. 8 shows that an increase in floodwater elevation from the levee crown
241 to the top of the wall results in a decrease in FS value. From Fig. 8(c) it can be concluded that the
242 steeper the landside slope of the levee is, the design experiences a lower factor of safety and at
243 high water elevation, the FS values are approximately close for variations of landside levee slope.

244 Figs. 9 and 10 show that the effects of the soil-related random variables, s_u of levee fill and
245 ϕ of sandy foundation, on FS are opposite to that of floodwater elevation. With levee fill of higher
246 s_u , the FS of designs with D_{mid} and D_{min} are similar, as shown in Fig. 9(a). Fig. 9(b) shows that the
247 I-walls and levee system with a wider levee crown gives a slightly greater FS, however by
248 increasing s_u the increase in FS is not significant for the three design cases (X_{min} , X_{mid} , X_{max}).
249 Generally, Fig. 9 indicates that the variation in s_u of the levee fill has a minor effect on the overall
250 stability of the system comparing to the other random variables. As shown in Fig. 10(a), at low ϕ

251 the FS of design with minimum wall depth is close to that of medium depth. From Figs. 10(b) and
252 10(c), it can be noticed that in terms of levee crown width and landside slope variation of FS with
253 a variation of φ follow similar trends. Overall, along with evaluating the variation of FS with
254 random variables, the observed variations of FS itself due to variations of uncertainties can provide
255 reasonable justification for selecting those governing random variables.

256 **4. RESPONSE SURFACE-BASED PROBABILISTIC EVALUATION OF I-WALLS AND**
257 **LEVEE SYSTEM**

258 **Response Surface for the I-Walls and Levee System**

259 The traditional probabilistic design approach requires numerous finite element simulations
260 and is computationally cumbersome (Goh et al. 2017; Zhang et al. 2019). The response surface
261 method (Wong 1985; Zhang et al. 2017; Zhang et al. 2020) is an efficient approach to express the
262 FS of the overall stability of the I-walls and levee system as a mathematical function of design
263 parameters and random variables. The response surface method has been demonstrated as an
264 effective tool for the reliability analysis of complex geotechnical problems through approximating
265 the implicit numerical solutions (e.g., finite element model) with explicit and computationally
266 efficient mathematical models (e.g., Wong 1985; Zhang et al. 2015; Zhang et al. 2020). Among
267 the common models used in the response surface method (Khuri and Mukhopadhyay 2010; Zhang
268 et al. 2015), the second-order polynomial model was used as shown below in this study:

269
$$y = b_0 + \sum_{i=1}^n b_i x_i + \sum_{i=1}^n b_{ii} x_i^2 \quad (2)$$

270 where y and x_i denote the response and input variables, respectively and b_0 , b_i and b_{ii} are the
271 coefficients determined from the central composite design based regression analysis. Using the

272 model in Eq. 2 via the regression analysis between the input variables and the response, the
 273 response surface to evaluate the FS for the overall stability of the I-walls and levee system can be
 274 determined as:

275

$$276 \quad FS = 0.7756 + 0.0134\phi + 0.0513s_u - 0.3324wl + 0.0554D + 0.0451X - 6.7437S \\ + 0.0013\phi^2 - 0.0006s_u^2 - 0.0559wl^2 + 0.0033D^2 + 0.0050X^2 + 5.4571S^2 \quad (3)$$

277 A number of random design sets combined with randomly selected uncertain parameters
 278 were generated to validate the response surface. The calculated FS values from the response
 279 surface were compared with those obtained from the finite element simulations, and the resulted
 280 coefficient of determination (R^2) value for the built response surface function equals to 0.968 (1.0
 281 being the highest possible value that indicates the perfect agreement). To evaluate the accuracy of
 282 the developed response surface quantitatively, three quantitative indicators recommended by
 283 Moriasi et.al (2007) were adopted for comparing the simulation results (i.e., results from SLIDE)
 284 with the observed results (i.e., results from response surface). The indicators used in this study are
 285 the Nash-Sutcliffe efficiency (NSE), the percent bias (PBIAS), and the ratio of the root mean
 286 square error to the standard deviation of measured data (RSR) that are shown in Eqs. 4, 5, and 6,
 287 respectively.

$$288 \quad NSE = 1 - \left[\frac{\sum_{i=1}^n (Y_i^{obs} - Y_i^{sim})^2}{\sum_{i=1}^n (Y_i^{obs} - Y_i^{mean})^2} \right] \quad (4)$$

$$289 \quad PBIAS = \left[\frac{\sum_{i=1}^n (Y_i^{obs} - Y_i^{sim}) * 100}{\sum_{i=1}^n Y_i^{obs}} \right] \quad (5)$$

$$290 \quad RSR = \frac{\left[\sqrt{\sum_{i=1}^n (Y_i^{obs} - Y_i^{sim})^2} \right]}{\left[\sqrt{\sum_{i=1}^n (Y_i^{obs} - Y_i^{mean})^2} \right]} \quad (6)$$

291 where Y^{obs} is the observation (FS from PLAXIS 2D), Y^{sim} is the simulated value (FS from response
 292 surface) and Y^{mean} is the mean of observed data. These validation statistics were computed, and the
 293 performance of the response surface was rated per Table 5. The overall performance was described
 294 as Very Good, and therefore, the mathematical model presented in Eq. 3 can be applied for
 295 computing FS for any combination of random and design parameters.

296 **Quantifying the Failure Probability of the System**

297 In the probabilistic design approach, the failure probability or other concepts such as the
 298 reliability index is used as a measure of safety. This paper evaluates the failure probability using
 299 the Monte Carlo simulations (MCS) based on the response surface in Eq. 2. The simulation is
 300 deemed to be in the failure region if the calculated FS is less than the required FS of 1.5. The soil-
 301 related random variables (φ, s_u) were assumed to be normally distributed as $\varphi = N(33, 1.67)$ and
 302 $s_u = N(31, 3.67)$ to evaluate the effect of random variables on P_f computation. It should be noted
 303 that the flood water elevation varies from the crown of the levee (0 m) to the wall top (2 m) and
 304 the variation of failure probability was monitored with floodwater elevation as the loading-related
 305 random variable.

306 As shown in Figs. 11-13, the maximum water elevations with acceptable P_f were 2 m, 1.7
 307 m and 1.3 m for cases D_{max} , D_{mid} and D_{min} (X and S at mid. value), respectively; 2 m, 1.8 m and
 308 1.5 m for cases X_{max} , X_{mid} and X_{min} (D and S at mid. value); and 2 m, 1.7 m and 1.1 m for cases S_{min} ,
 309 S_{mid} and S_{max} (D and X at mid. value), respectively.

310 Overall, it can be concluded from Figs. 11-13 that P_f of the I-walls and levee system
311 decreases with increasing D , increasing X and decreasing S . Moreover, based on the allowable
312 failure probability of 0.01 (Jonkman et al. 2009), the design combinations that satisfy this safety
313 constraint are: $(D_{max}, X_{mid}, S_{mid})$, $(D_{mid}, X_{max}, S_{mid})$, $(D_{mid}, X_{mid}, S_{min})$. However, more design sets
314 can be generated that meet the safety criteria by adjusting the design parameters. For example,
315 although D_{min} in a design set causes the failure probability of the system exceeding the allowable
316 one, the combination of D_{min} with X_{max} and S_{min} can result in satisfactory performance of the system.

317 **5. DESIGN OPTIMIZATION FOR STABILITY OF I-WALLS AND LEVEE SYSTEM**

318 **Non-Robust Design Optimization Results**

319 The design optimization was firstly performed to minimize both the cost and the failure
320 probability using the multi-objective optimization procedures (Deb et al. 2002; Yu et al. 2019).
321 The cost of I-walls and levee system is expressed as a function of the design parameters (D , X and
322 S) based on the construction volume of each component and respective unit cost data by RSmeans
323 (Waier et al. 2010; Rahbari and Ravichandran 2018). It should be noted that in this type of design
324 optimization, robustness was not considered, and only cost and safety were considered as two
325 design objectives. The failure probability is evaluated using Monte Carlo simulation with the total
326 sample number $N = 5000$. As a safety constraint, an allowable P_f equal to 0.01 was assumed in the
327 optimization setting. The resulted Pareto front shows a trade-off relationship between cost
328 efficiency (minimizing the cost) and safety (minimizing the failure probability), which is depicted
329 as a non-robust Pareto Front in Fig. 15.

330 **Robust Design Optimization Results**

331 Certainty in the computation of the failure probability of the system may be guaranteed by
332 using high-quality data of the soil profile in the model. However, uncertainties exist in the assumed
333 statistical characterization of soil properties due to insufficient sample size, measurement errors,
334 and human errors and the computed failure probability will not be a certain value and vary under
335 the effect of these variations (Rahbari 2017; Luo and Hu 2019; Wu and Luo 2020). Therefore, in
336 this section, the coefficient of variations (COV) of the soil-related random variables (φ and s_u)
337 were also considered as uncertain parameters in the optimization setting as $\text{COV}_\varphi = N(0.05, 0.01)$,
338 $\text{COV}_{s_u} = N(0.12, 0.024)$.

339 For each design set, M number of P_f were calculated (note: M is the number of MCS runs
340 to obtained the standard deviation of P_f). Considering P_f as the response of concern, the standard
341 deviation of P_f was taken as the measure of robustness (Wang et al. 2015). The design optimization
342 was performed by minimizing the cost and maximizing the robustness. Reducing the variation of
343 response (standard deviation of the failure probability, here) leads to increasing the robustness of
344 the design. The Pareto front optimized to cost and standard deviation of P_f is shown in Fig. 14 (for
345 $M=1000$). It can be observed from the Fig. that as the standard deviation of P_f increased from 0 to
346 about 0.0017, the cost decreased from \$2800 to \$1900. This indicates that higher robustness for
347 design demands a higher cost.

348 **Comparison of Robust and Non-Robust Design Optimization**

349 In this section, the Pareto front resulted from robust design optimization is compared with
350 the one resulted from non-robust design optimization, as shown in Fig. 15. The non-robust Pareto
351 front is located below the robust Pareto front showing the lower cost of design when the robustness

352 of the system is not considered. In other words, robust design optimization may lead to costlier
353 designs than non-robust design, but reducing the sensitivity of the design and the variation of the
354 response (failure probability) is the key to obtain designs of higher robustness.

355 **Determination of Final Design**

356 To identify the most preferred design on the Pareto front, the normal boundary intersection
357 (NBI) (Das and Dennis, 1998) approach was used to compute the knee points on the robust Pareto
358 front. As shown in Fig. 16, for each point of the Pareto front, the distance from the boundary line,
359 which connects the highest point of the Pareto front to the lowest point, is computed in the
360 normalized space of the Pareto front. Then, the point with maximum distance from the boundary
361 line is sought and selected as the knee point which corresponds to the most preferred design of the
362 study based on the gain-sacrifice relationship among the designs on the Pareto front.

363 The most preferred designs (D , X , S , and associated cost) extracted using the knee point
364 characteristics of the robust and non-robust design Pareto fronts are summarized in Table 6. The
365 most preferred robust design included a levee with a wide crown and mild slope for the levee
366 landside and short wall. On the other hand, the most preferred non-robust design included a levee
367 with a middle-value width for the crown. From the comparison study, a mild slope (about 4H:1V)
368 for the levee landside is recommended for the final design of I-walls and levee system. The levee
369 crown's increased width in the most preferred robust design increased the cost of the system.
370 However, in the meantime, the robustness of the design also increased considerably. This higher
371 cost for the robust design may seem unreasonable compared to conventional design, but the robust
372 design helps to reduce the unexpected variations in the system response. The proposed robust
373 design optimization framework will assist the designers to make a more informed decision by
374 explicitly considering the safety, cost, and robustness.

375 **6. CONCLUSION**

376 A general framework for designing and optimizing I-walls and levees system resting on
377 sandy foundation soil is proposed. The uncertainties associated with the geotechnical properties
378 and loads from the flood water are systematically considered. The stability of I-walls and levee
379 system was evaluated using finite element and limit equilibrium methods, and a response surface
380 for the factor of safety was developed based on the computed results. Then, using the formulated
381 response surface, the failure probability was determined using Monte Carlo simulations. A multi-
382 objective design optimizations were conducted to derive the non-robust Pareto front (cost vs.
383 failure probability) and robust Pareto front (cost vs. standard deviation of the failure probability).
384 The robust design framework optimizes the robustness (in terms of minimizing the standard
385 deviation of the failure probability) and cost-efficiency (in terms of minimizing the cost)
386 simultaneously while satisfying the safety requirements. The robust design framework can be
387 directly used to design I-walls and levees system resting on sandy soil for its stability to mitigate
388 the risk of catastrophic failures caused by geotechnical and floodwater uncertainties.

389 **ACKNOWLEDGMENTS**

390 This research was supported by Glenn Department of Civil Engineering, Clemson
391 University. The second author also wishes to acknowledge the support from the National Science
392 Foundation (Award 1818649 and 1900445). The results and opinions expressed in this paper do
393 not necessarily reflect the views and policies of the National Science Foundation.

394

395 **REFERENCES**

396 Brinkgreve RBJ, Kumarswamy S, Swolfs WM (2015) Plaxis 2D Manual. *PLAXIS bv, The*
397 *Netherlands.*

398 Burk & Associates, Inc (1986) London avenue canal floodwalls and levees – General design
399 memorandum.

400 Chen JF, Liu JX, Xue JF, Shi ZM (2014) Stability analyses of a reinforced soil wall on soft soils
401 using the strength reduction method. *Engineering Geology*, 177, 83-92, DOI:
402 10.1016/j.enggeo.2014.05.018

403 Chen Z, Du J, Yan J, Sun P, Li K, Li Y (2019) Point estimation method: Validation, efficiency
404 improvement, and application to embankment slope stability reliability analysis. *Engineering*
405 *Geology*, 105232, DOI: 10.1016/j.enggeo.2019.105232

406 Coduto DP (1999) Geotechnical engineering: principles and practices. Prentice Hall, Upper Saddle
407 River, NJ, USA.

408 Das B (2010) Principles of Geotechnical Engineering. Cengage Learning, Boston, MA, USA.

409 Das I, Dennis J E (1998) Normal-boundary intersection: A new method for generating the Pareto
410 surface in nonlinear multi-criteria optimization problems. *SIAM Journal on*
411 *Optimization*, 8(3), 631-657, DOI: 10.1137/S1052623496307510

412 Dunbar JB, Britsch III LD (2008) Geology of the New Orleans area and the canal levee failures.
413 *Journal of Geotechnical and Geoenvironmental Engineering*, 134(5), 566-582, DOI:
414 10.1061/(ASCE)1090-0241(2008)134:5(566)

415 Duncan JM (2000) Factors of safety and reliability in geotechnical engineering. *Journal of*
416 *Geotechnical and Geoenvironmental Engineering*, 126(4), 307-316, DOI:
417 10.1061/(ASCE)1090-0241(2000)126:4(307)

418 Duncan JM, Brandon TL, Wright SG, Vroman N (2008) Stability of I-walls in New Orleans during
419 hurricane Katrina. *Journal of Geotechnical and Geoenvironmental Engineering*, 134(5), 681-
420 691, DOI: 10.1061/(ASCE)1090-0241(2008)134:5(681)

421 Flor A, Pinter N, Remo JW (2010) Evaluating levee failure susceptibility on the Mississippi River
422 using logistic regression analysis. *Engineering Geology*, 116(1-2), 139-148, DOI:
423 10.1016/j.enggeo.2010.08.003

424 Gao X, Liu H, Zhang W, Wang W, Wang Z (2019) Influences of reservoir water elevation
425 drawdown on slope stability and reliability analysis. *Georisk: Assessment and Management of*
426 *Risk for Engineered Systems and Geohazards*, 13(2), 145-153. DOI:
427 10.1080/17499518.2018.1516293

428 Goh ATC, Zhang F, Zhang W, Zhang Y, Liu H (2017) A simple estimation model for 3D braced
429 excavation wall deflection. *Computers and Geotechnics*, 83, 106-113, DOI:
430 10.1016/j.compgeo.2016.10.022

431 Gong W, Khoshnevisan S, Juang CH (2014) Gradient-based design robustness measure for robust
432 geotechnical design. *Canadian Geotechnical Journal*, 51(11), 1331-1342, DOI: 10.1139/cgj-
433 2013-0428

434 Griffiths DV, Lane PA (1999) Slope stability analysis by finite elements. *Geotechnique*, 49(3),
435 387-403, DOI: 10.1680/geot.1999.49.3.387

436 Hui R (2014) Optimal design of levee and flood control systems. Doctoral dissertation, University
437 of California, Davis, USA.

438 Interagency Performance Evaluation Task Force IPET (2007) Performance evaluation of the New
439 Orleans and Southeast Louisiana Hurricane protection system. Final Rep. of the Interagency
440 Performance Evaluation Task Force, United States Army Corps of Engineers, Washignton DC,
441 USA.

442 Ji J (2014) A simplified approach for modeling spatial variability of undrained shear strength in
443 out-plane failure mode of earth embankment. *Engineering Geology*, 183, 315-323, DOI:
444 10.1016/j.enggeo.2014.09.004

445 Jonkman SN, Kok M, Van Ledden M, Vrijling JK (2009) Risk-based design of flood defence
446 systems: a preliminary analysis of the optimal protection level for the New Orleans
447 metropolitan area. *Journal of Flood Risk Management*, 2(3), 170-181, DOI: 10.1111/j.1753-
448 318X.2009.01036.x

449 Liu Y, Zhang W, Zhang L, Zhu Z, Hu J, Wei H (2018) Probabilistic stability analyses of undrained
450 slopes by 3D random fields and finite element methods. *Geoscience Frontiers*, 9(6), 1657-
451 1664, DOI: 10.1016/j.gsf.2017.09.003

452 Luo Z, Hu B (2019) Robust design of energy piles using a fuzzy set-based point estimate method.
453 *Cold Regions Science and Technology*, 168, 102874, DOI: 10.1016/j.coldregions.2019.102874

454 Moriasi DN, Arnold JG, Van Liew MW, Bingner RL, Harmel RD, Veith TL (2007) Model
455 evaluation guidelines for systematic quantification of accuracy in watershed
456 simulations. *Transactions of the ASABE*, 50(3), 885-900, DOI: 10.13031/2013.23153

457 Rahbari P, Ravichandran N (2018) Design Optimization of I-Wall Levee System Supported by
458 Sand Foundation. Proceedings of International Foundations Congress & Equipment Expo
459 (IFCEE 2018), March 5-10, Orlando, FL, USA.

460 Sasanakul I, Vanadit-Ellis W, Sharp M, Abdoun T, Ubilla J, Steedman S, Stone K (2008) New
461 Orleans levee system performance during Hurricane Katrina: 17th Street Canal and Orleans
462 Canal North. *Journal of Geotechnical and Geoenvironmental Engineering*, 134(5), 657-667,
463 DOI: 10.1061/(ASCE)1090-0241(2008)134:5(657)

464 Seed RB, Bea RG, Abdelmalak RI, Athanasopoulos AG, Boutwell Jr GP, Bray JD, Briaud JL,
465 Cheung C, Cobos-Roa D, Cohen-Waeber J, Collins BD (2006) Investigation of the
466 Performance of the New Orleans Flood Protection System in Hurricane Katrina on August 29,
467 2005. Independent Levee Investigation Team: Final Report.

468 Sills G L, Vroman ND, Wahl RE, Schwanz NT (2008) Overview of New Orleans levee failures:
469 lessons learned and their impact on national levee design and assessment. *Journal of
470 Geotechnical and Geoenvironmental Engineering*, 134(5), 556-565, DOI:
471 10.1061/(ASCE)1090-0241(2008)134:5(556)

472 Tan X, Shen M, Juang CH, Zhang Y (2020) Modified robust geotechnical design approach based
473 on the sensitivity of reliability index. *Probabilistic Engineering Mechanics*, 60, 103049, DOI:
474 10.1016/j.probengmech.2020.103049

475 Tung YK, Mays LW (1981) Risk models for flood levee design. *Water Resources Research*, 17(4),
476 833-841, DOI: 10.1029/WR017i004p00833

477 Ubilla J, Abdoun T, Sasanakul I, Sharp M, Steedman S, Vanadit-Ellis W, Zimmie T (2008) New
478 Orleans levee system performance during hurricane Katrina: London Avenue and Orleans
479 canal south. *Journal of Geotechnical and Geoenvironmental Engineering*, 134(5), 668-680,
480 DOI: 10.1061/(ASCE)1090-0241(2008)134:5(668)

481 USACE (2011) EC 1110-2-6066, Engineering and design: Design of I-walls. United States Army
482 Corps of Engineers, Washington DC, USA.

483 USACE (2000) EM-1110-2-1913, Engineering and design: Design and construction of levees.
484 United States Army Corps of Engineers, Washington DC, USA.

485 Waier PR, Babbitt C, Baker T, Balboni B, Bastoni RA (2010) RSMeans: Building Construction
486 Cost Data 2010.

487 Wong FS (1985) Slope reliability and response surface method. *Journal of Geotechnical
488 Engineering*, 111(1), 32-53, DOI: 10.1061/(ASCE)0733-9410(1985)111:1(32)

489 Wright SG, Duncan JM (2005) Soil Strength and Slope Stability. John Wiley & Sons, Hoboken,
490 NJ, USA.

491 Wu Z, Luo Z (2020) Life-Cycle System Reliability-Based Approach for Bridge Pile Foundations
492 under Scour Conditions. *KSCE Journal of Civil Engineering*, 24(2), 412-423, DOI:
493 10.1007/s12205-020-0916-2

494 Yang MD, Lin JY, Yao CY, Chen JY, Su TC, Jan CD (2011) Landslide-induced levee failure by
495 high concentrated sediment flow—A case of Shan-An levee at Chenyulan River, Taiwan.
496 *Engineering Geology*, 123(1-2), 91-99, DOI: 10.1016/j.enggeo.2011.07.006

497 Yu Y, Shen M, Juang CH (2019) Assessing Initial Stiffness Models for Laterally Loaded Piles in
498 Undrained Clay: Robust Design Perspective. *Journal of Geotechnical and Geoenvironmental
499 Engineering*, 145(10), 04019073, DOI: 10.1061/(ASCE)GT.1943-5606.0002074

500 Yu Y, Shen M, Sun H, Shang Y (2019) Robust design of siphon drainage method for stabilizing
501 rainfall-induced landslides. *Engineering Geology*, 249, 186-197, DOI:
502 10.1016/j.enggeo.2019.01.001

503 Zhang J, Chen HZ, Huang HW, Luo Z (2015) Efficient response surface method for practical
504 geotechnical reliability analysis. *Computers and Geotechnics*, 69, 496-505, DOI:
505 10.1016/j.compgeo.2015.06.010

506 Zhang J, Wang H, Huang HW, Chen LH (2017) System reliability analysis of soil slopes stabilized
507 with piles. *Engineering Geology*, 229, 45-52, DOI: 10.1016/j.enggeo.2017.09.009

508 Zhang W, Zhang R, Wang W, Zhang F, Goh ATC (2019) A multivariate adaptive regression
509 splines model for determining horizontal wall deflection envelope for braced excavations in
510 clays. *Tunnelling and Underground Space Technology*, 84, 461-471, DOI:
511 10.1016/j.tust.2018.11.046

512 Zhang W, Zhang R, Wu C, Goh ATC, Lacasse S, Liu Z, Liu H (2020) State-of-the-art review of
513 soft computing applications in underground excavations. *Geoscience Frontiers*, 11(4), 1095-
514 1106, DOI: 10.1016/j.gsf.2019.12.003

515

List of Figures

Figure 1 Expanding levee section

Figure 2 Common floodwalls: (a) I-walls and (b) T-walls (from USACE 2011)

Figure 3 The layout of the I-walls and levee system

Figure 4 A sample SLIDE model of I-walls and levee system

Figure 5 Dimensions of concrete cap of the I-walls

Figure 6 Sample finite element model of I-walls and levee system

Figure 7 Comparison of FS from FE: PLAXIS 2D and FS from LE: SLIDE (Spencer)

Figure 8 Variation of FS with flood water level (a: effects of embedded depth of wall D ; b: effects of levee crown width X ; c: effects of slope ratio of the landside S)

Figure 9 Variation of FS with undrained shear strength of levee fill (a: effects of embedded depth of wall D ; b: effects of levee crown width X ; c: effects of slope ratio of the landside S)

Figure 10 Variation of FS with friction angle of sand foundation (a: effects of embedded depth of wall D ; b: effects of levee crown width X ; c: effects of slope ratio of the landside S)

Figure 11 Variation of P_f with flood water level considering D

Figure 12 Variation of P_f with flood water level considering X

Figure 13 Variation of P_f with flood water level considering S

Figure 14 Robust Pareto front optimized to cost and standard deviation of failure probability

Figure 15 Comparison of robust and non-robust Pareto fronts

Figure 16 Normal boundary intersection approach

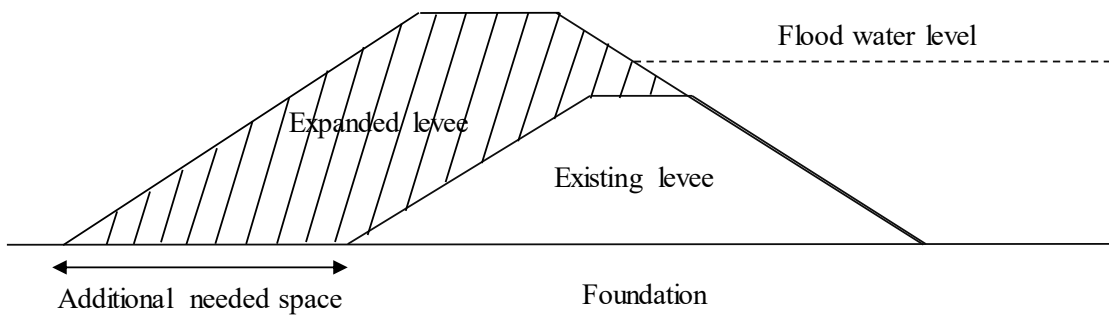


Figure 1 Expanding levee section

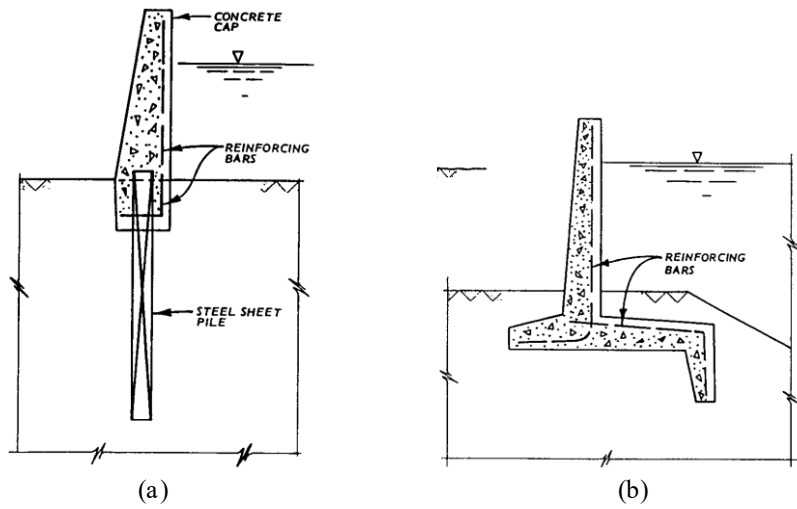


Figure 2 Common floodwalls: (a) I-walls and (b) T-walls (from USACE 2011)

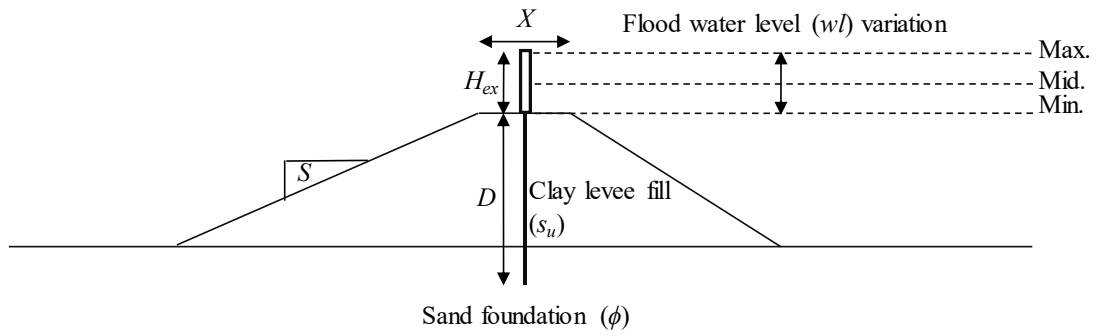


Figure 3 The layout of the I-walls and levee system

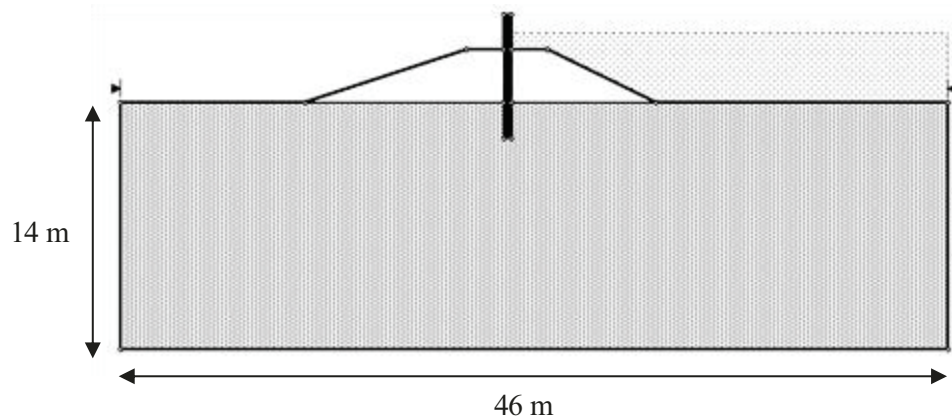


Figure 4 A sample SLIDE model of I-walls and levee system

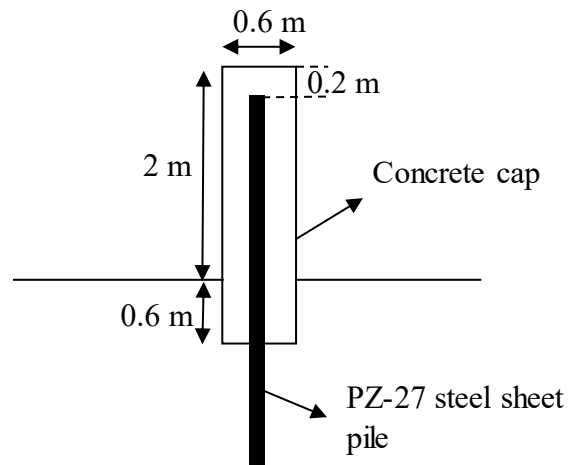


Figure 5 Dimensions of concrete cap of the I-walls

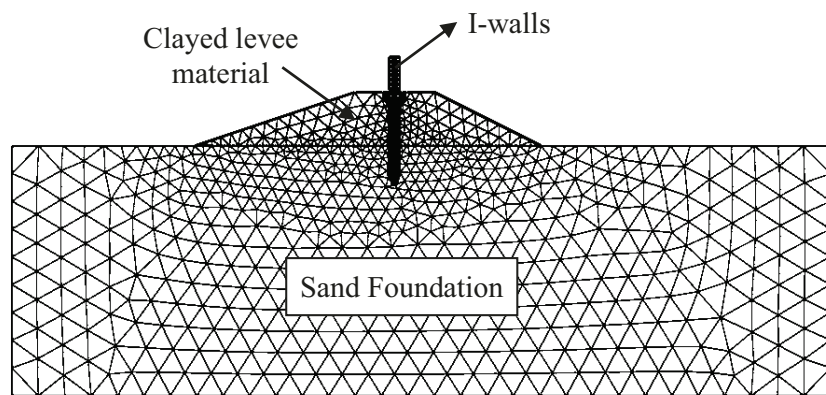


Figure 6 Sample finite element model of I-walls and levee system

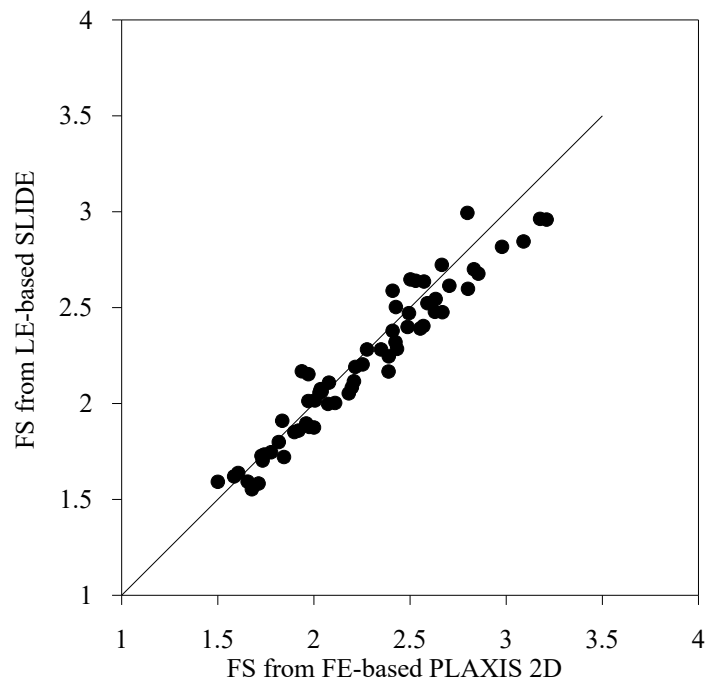


Figure 7 Comparison of FS from FE: PLAXIS 2D and FS from LE: SLIDE (Spencer)

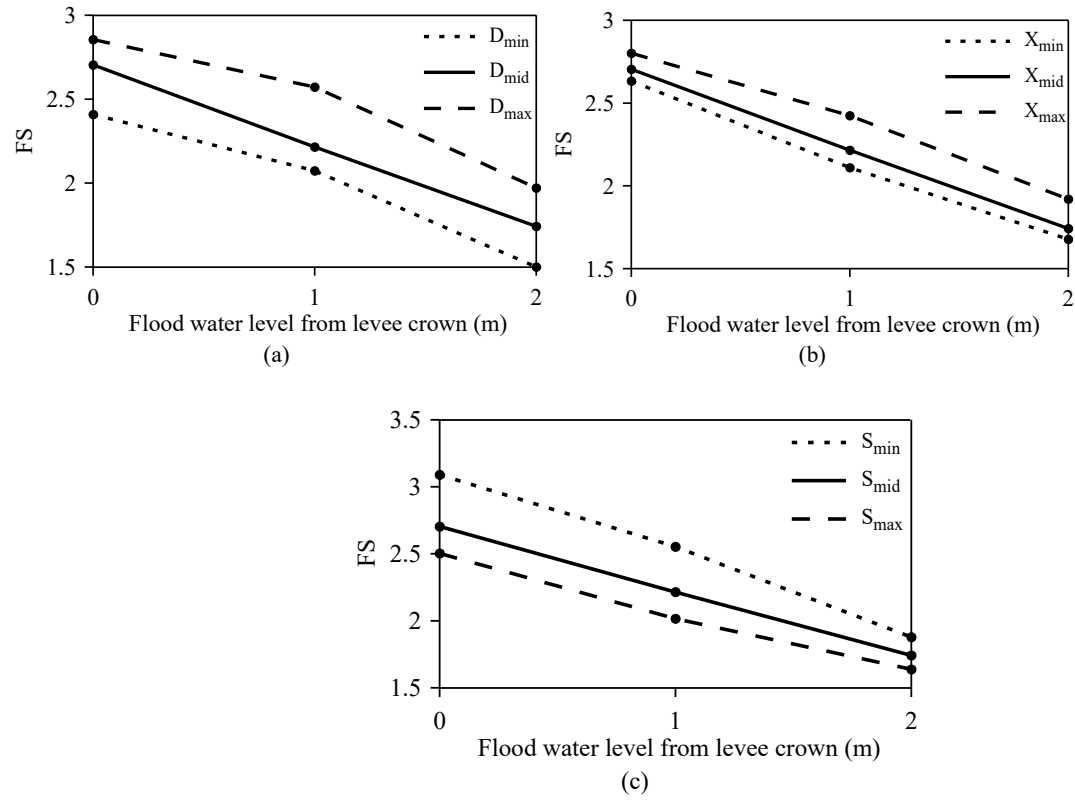


Figure 8 Variation of FS with flood water level (a: effects of embedded depth of wall D ; b: effects of levee crown width X ; c: effects of slope ratio of the landside S)

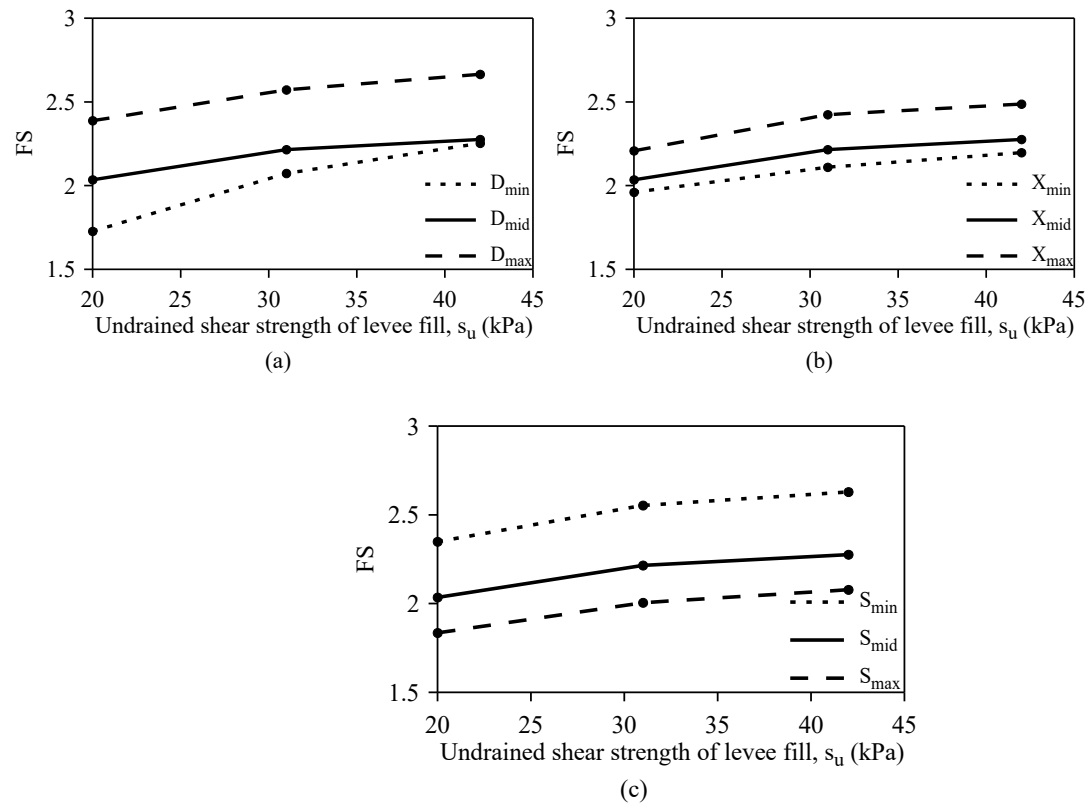


Figure 9 Variation of FS with undrained shear strength of levee fill (a: effects of embedded depth of wall D ; b: effects of levee crown width X ; c: effects of slope ratio of the landside S)

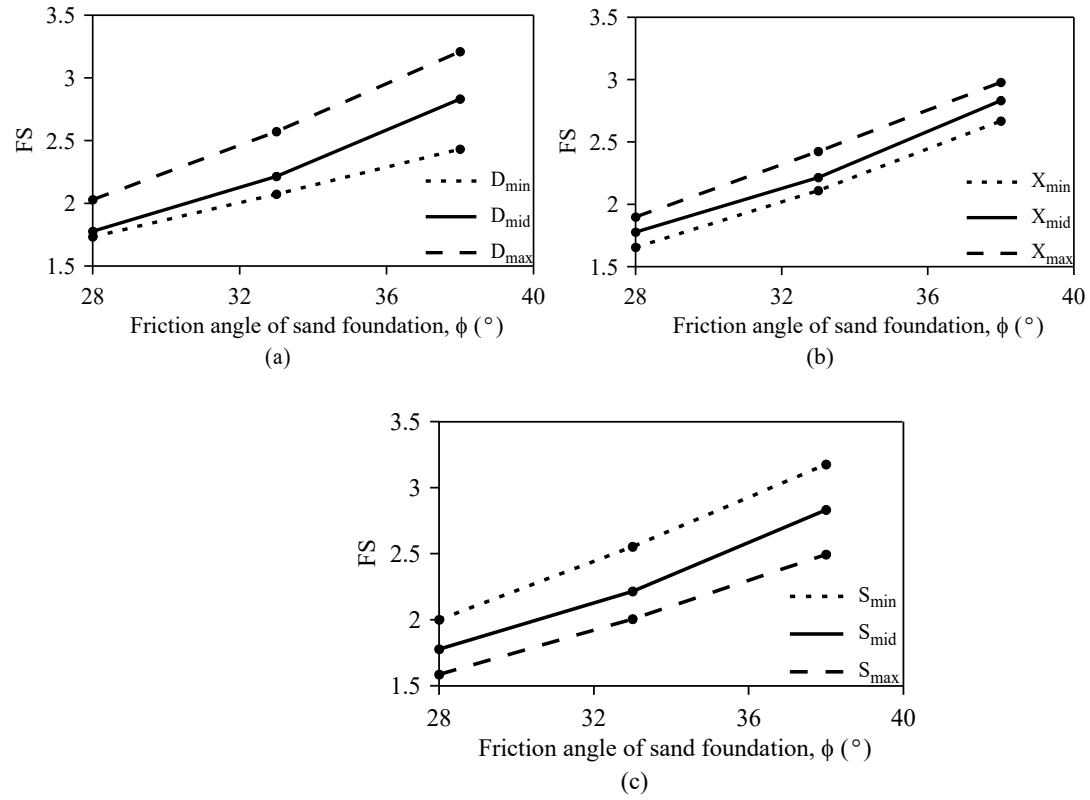


Figure 10 Variation of FS with friction angle of sand foundation (a: effects of embedded depth of wall D ; b: effects of levee crown width X ; c: effects of slope ratio of the landside S)

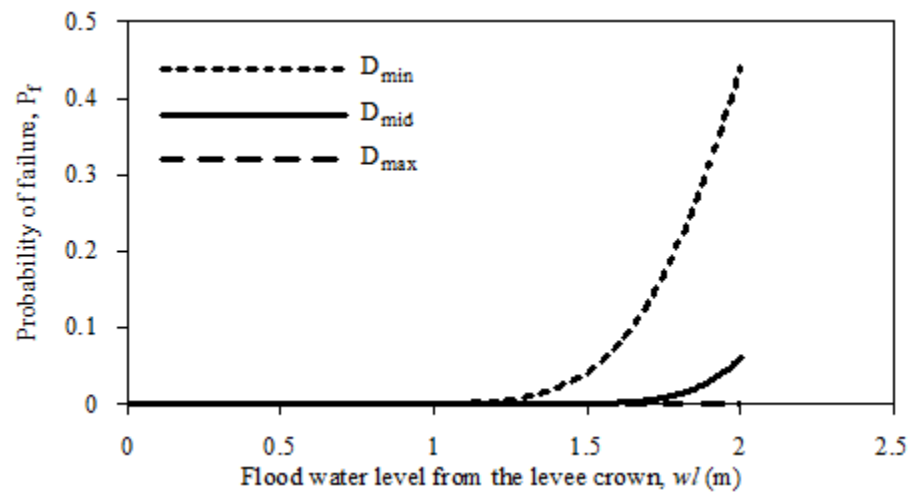


Figure 11 Variation of P_f with flood water level considering D

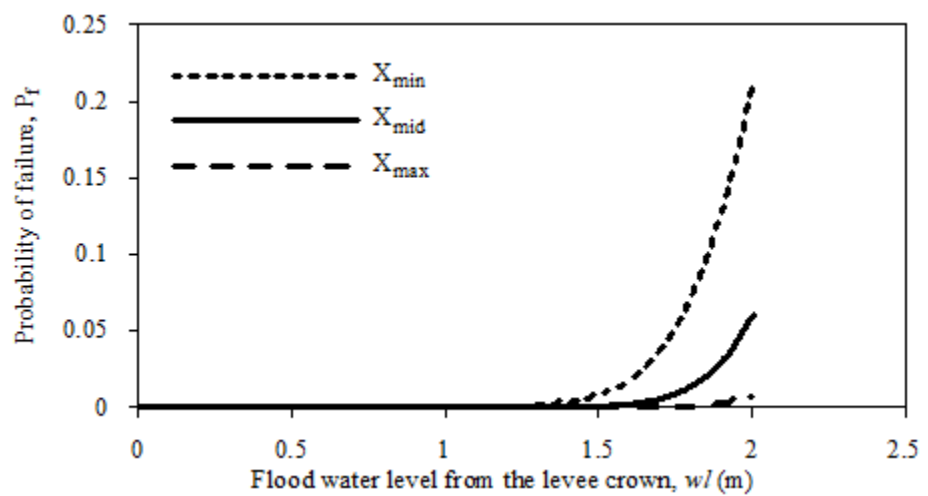


Figure 12 Variation of P_f with flood water level considering X

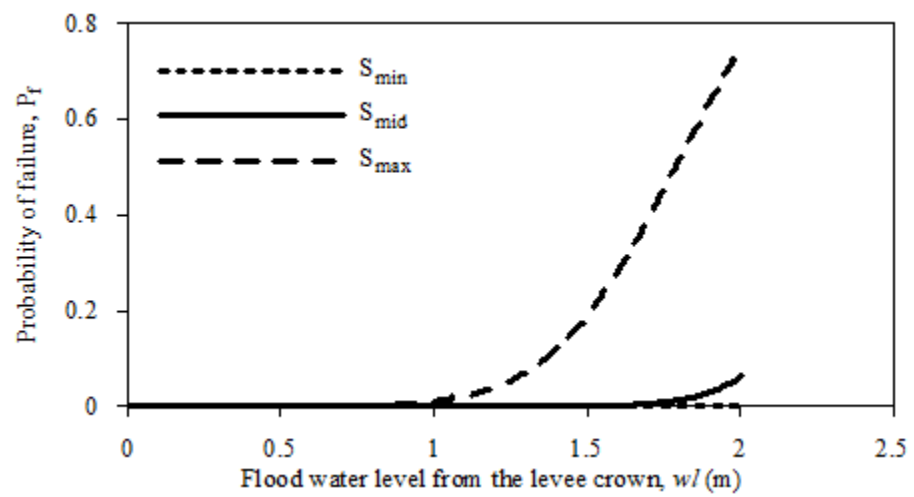


Figure 13 Variation of P_f with flood water level considering S

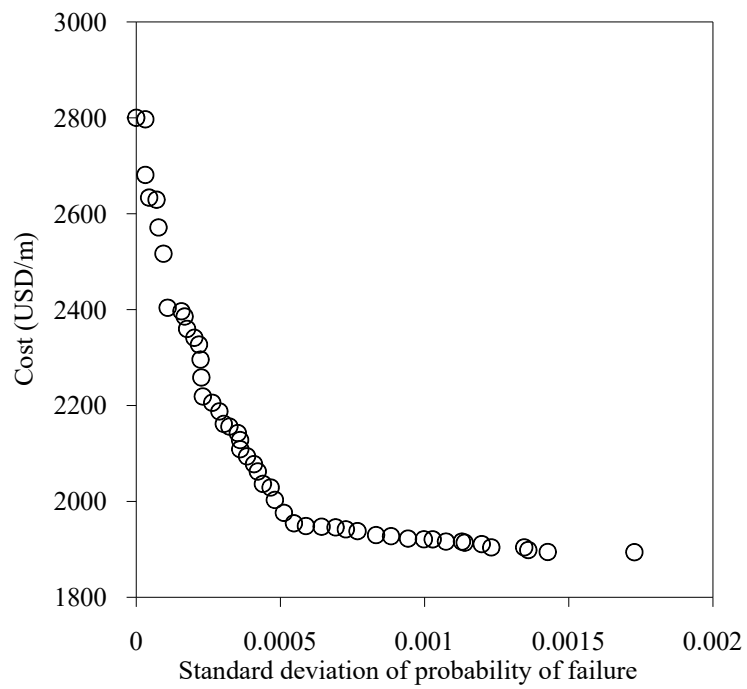


Figure 14 Robust Pareto front optimized to cost and standard deviation of failure probability

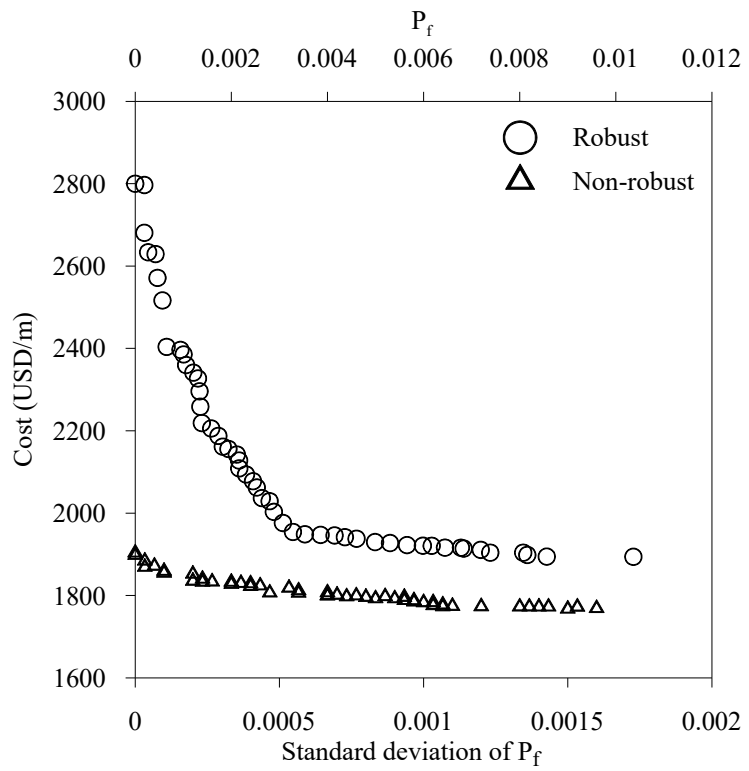


Figure 15 Comparison of robust and non-robust Pareto fronts

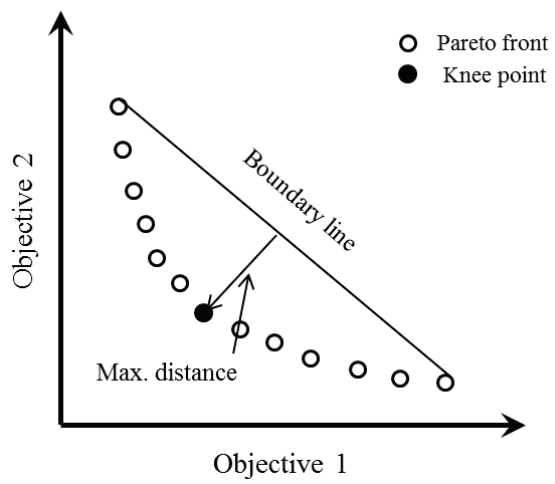


Figure 16 Normal boundary intersection approach

List of Tables

Table 1 Design variables in the study

Table 2 Random variables and their statistical values

Table 3 Material properties of the sheet pile wall using PZ-27

Table 4 Selected design combinations for parametric study

Table 5 Performance ratings for recommended statistics (after Moriasi et al. 2007)

Table 6 Design parameters of the most preferred design for robust and non-robust optimization

Table 1 Design variables in the study

Design variable	Wall embedded depth, D (m)	Levee crown width, X (m)	Levee landside slope, S
Range	2-8	3-6	0.25-0.5

Table 2 Random variables and their statistical values

Random variable	Range	Mean value	Standard deviation
φ (°)	28-38	33	1.67
s_u (kPa)	20-42	31	3.67
wl (m)	0-2	1	-

Table 3 Material properties of the sheet pile wall using PZ-27

PZ-27	Parameter	Unit	Value
From Bethlehem steel corporation	h	mm	305
	A	cm^2/m	168.1
	weight	kg/m^2	131.8
	I	cm^4/m	25200
	$EA (= E(hb))$	kN/m	3.362×10^6
Used in PLAXIS 2D	$EI (= E \left(\frac{bh^3}{12} \right))$	$\text{kN} \cdot \text{m}^2/\text{m}$	5.04×10^4
	$d (= h = \sqrt{12 \left(\frac{I}{A} \right)})$	m	0.4241
	$w (= \text{weight} \times g \times 10^{-3})$	kN/m/m	1.293

Table 4 Selected design combinations for parametric study

Combination	D (m)	X (m)	S
$D_{mid}, X_{mid}, S_{mid}$	5	4.5	0.33
$D_{min}, X_{min}, S_{min}$	2	3	0.25
$D_{max}, X_{max}, S_{max}$	8	6	0.5
$D_{min}, X_{mid}, S_{mid}$	2	4.5	0.33
$D_{max}, X_{mid}, S_{mid}$	8	4.5	0.33
$D_{mid}, X_{min}, S_{mid}$	5	3	0.33
$D_{mid}, X_{max}, S_{mid}$	5	6	0.33
$D_{mid}, X_{mid}, S_{min}$	5	4.5	0.25
$D_{mid}, X_{mid}, S_{max}$	5	4.5	0.5

Table 5 Performance ratings for recommended statistics (after Moriasi et al. 2007)

Performance rating	RSR	NSE	PBIAS
Very Good	0-0.5	0.75-1	<±15
Good	0.5-0.6	0.65-0.75	±15 - ±30
Satisfactory	0.6-0.7	0.5-0.65	±30 - ±55
Unsatisfactory	>0.7	<0.5	>±55
Response surface rating	0.24	0.94	-0.36

Table 6 Design parameters of the most preferred design for robust and non-robust optimization

Optimization type	D (m)	X (m)	S	Cost (USD/m)
Robust	2.00	6.00	0.25	1954
Non-robust	2.00	3.55	0.28	1807